



Contents lists available at ScienceDirect

Bioorganic & Medicinal Chemistry Letters

journal homepage: www.elsevier.com/locate/bmcl

Aleglitazar, a new, potent, and balanced dual PPAR α / γ agonist for the treatment of type II diabetes

Agnes Bénardeau^a, Jörg Benz^a, Alfred Binggeli^a, Denise Blum^a, Markus Boehringer^a, Uwe Grether^a, Hans Hilpert^a, Bernd Kuhn^a, Hans Peter Märki^a, Markus Meyer^b, Kurt Püntener^a, Susanne Raab^a, Armin Ruf^a, Daniel Schlatter^a, Peter Mohr^{a,*}

^a F. Hoffmann-La Roche Ltd, Pharma Research, CH-4070 Basel, Switzerland

^b F. Hoffmann-La Roche Ltd, Pharma Development, CH-4070 Basel, Switzerland

ARTICLE INFO

Article history:

Received 12 February 2009

Revised 11 March 2009

Accepted 12 March 2009

Available online 14 March 2009

Keywords:

α -Alkoxypropionic acids

Nuclear hormone receptors

PPAR

X-ray crystallography

Diabetes

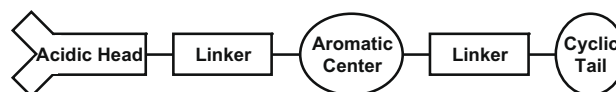
Dyslipidemia

ABSTRACT

Design, synthesis, and SAR of novel α -alkoxy- β -arylpropionic acids as potent and balanced PPAR α / γ coagonists are described. One representative thereof, Aleglitazar ((**S**)-**2Aa**), was chosen for clinical development. Its X-ray structure in complex with both receptors as well as its high efficacy in animal models of T2D and dyslipidemia are also presented.

© 2009 Elsevier Ltd. All rights reserved.

Peroxisome Proliferator-Activated Receptors (PPAR) α , γ , and δ are three of the 48 nuclear hormone receptors encoded in the human genome.¹ As ligand-activated transcription factors they work in concert with co-activators and co-repressors and regulate gene expression.² PPAR α is supposed to control mainly genes involved in fatty acid β -oxidation and to play a pivotal role in energy homeostasis,³ whereas PPAR γ agonists seem to be mainly involved in glucose homeostasis, insulin sensitivity, and lipid storage.⁴ Ligands for the former, albeit very weak ones, generally termed Fibrates, have been in clinical use since a long time to treat dyslipidemia,⁵ whereas the glitazones (thiazolidinediones), agonists of the latter, belong today to the standard repertoire for type II diabetes treatment.⁶ The function of PPAR δ , on the other hand, is much less understood to date, but some recent data enlighten its role in the regulation of fatty acid oxidation in several tissues.⁷ Some time ago we reported about structure-based design and synthesis of indole propionic acids as novel PPAR α / γ coagonists.⁸ In this Letter we describe an extension of this work culminating in the discovery of Aleglitazar, a balanced, potent coagonist which provides new opportunities to address both hyperglycemia as well as the enhanced cardiovascular risk of diabetic patients.^{9,10} Aleglitazar has successfully completed phase II clinical development.



Scheme 1. Simplified topology of typical synthetic PPAR agonists. The linkers can be branched to access additional subpockets in the receptor.

Again, we started with a modular approach as schematically depicted in **Scheme 1**. We chose α -alkoxyacids, which are apt to form up to 4 pivotal hydrogen bonds with serine, tyrosine and histidine of the protein, as the acidic warhead; such a strong hydrogen acceptor is indispensable for obtaining potent agonists. For the cyclic tail, partly solvent exposed and in general quite tolerant with respect to structural variations, we focused again on the aryloxazole-moiety, present and well-tried in countless PPAR ligands like Farglitazar, Imiglitazar, or Muraglitazar, to name just a few. Regarding the aromatic center, close inspection of several X-ray structures revealed that a simple phenyl ring does not optimally fit the cavity of the receptor. We therefore decided to explore the potential of bicyclic cores, specifically naphthalene and benzothio-phene analogues which had already proven in the past, albeit restricted to pure PPAR γ agonists, to yield drug like antidiabetic compounds like Edaglitazone **1**. In the following, we describe the synthesis, SAR, X-ray structures, and in vivo activity of PPAR α / γ coagonists of generic structure **2**, **3**, and **4** (**Fig. 1**).

* Corresponding author. Tel.: +41 61 688 5691; fax: +41 61 688 64 59.
E-mail address: peter.mohr@roche.com (P. Mohr).

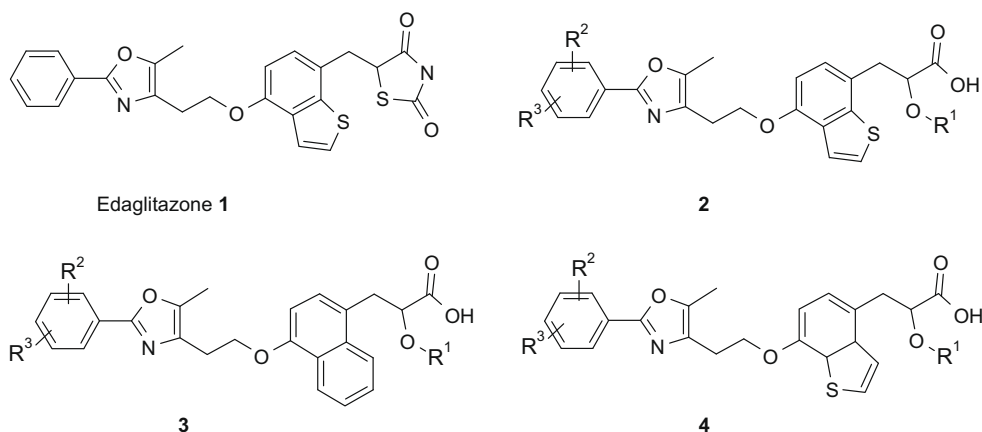
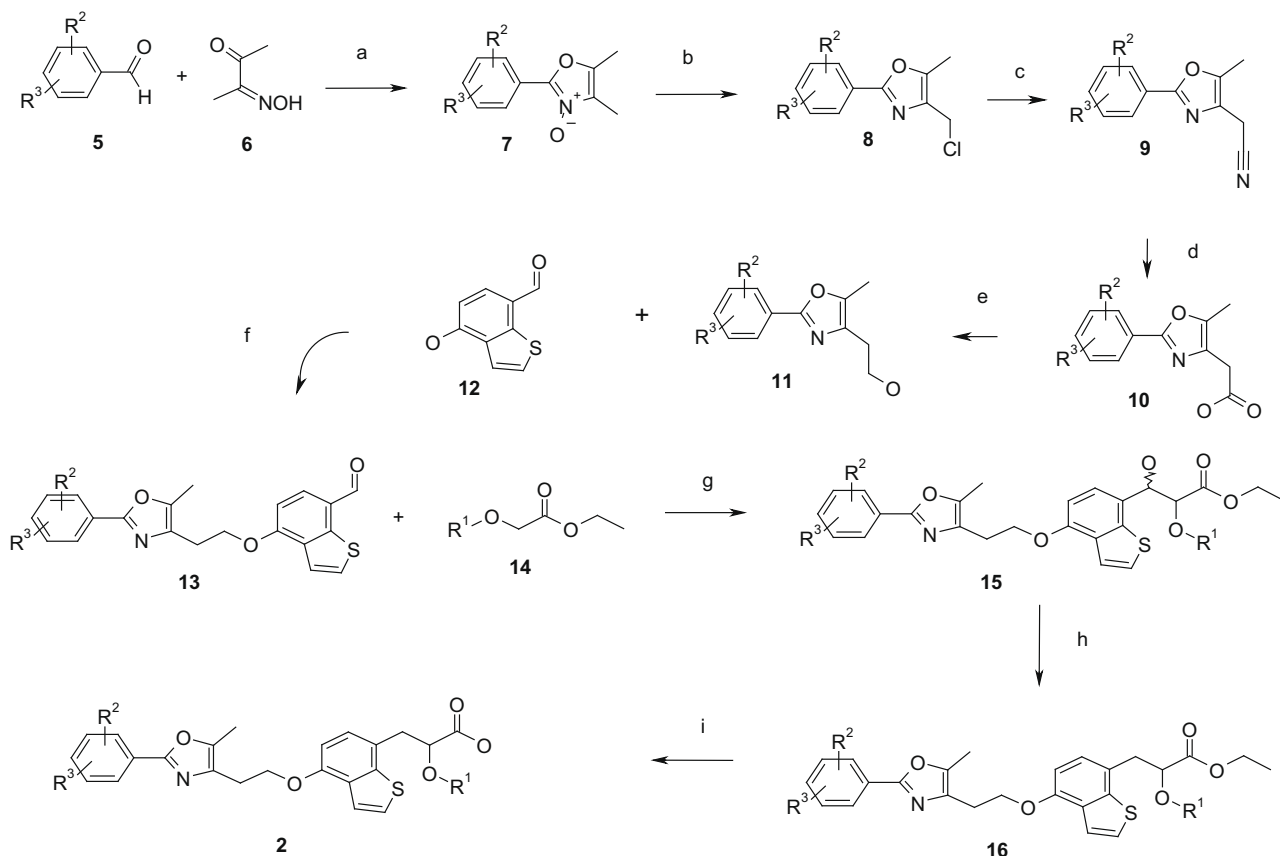


Figure 1. Chemical structure of Edaglitazone and PPAR coagonists **2–4**.

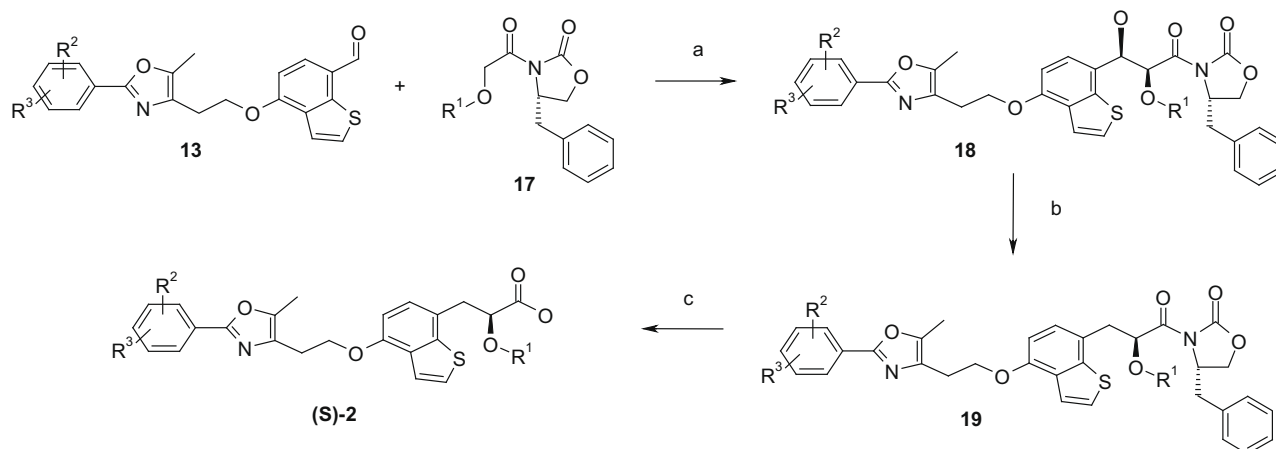
The synthesis started with the preparation of aryl-oxazoles **8** following the established route⁸ from the appropriate benzaldehyde **5** and butane-2,3-dione mono-oxime **6** via **7** according to Go-to's method (Scheme 2).¹¹ Elongation by one carbon atom to **9** was achieved by treatment with NaCN in DMSO. Standard hydrolysis and ensuing reduction of the carboxylic acid **10** with borane delivered the terminal alcohol **11**. Mitsunobu condensation with building block **12** generated finally the key intermediate **13**, albeit in moderate yield. The former was synthesized in an expeditious manner following the route described previously.¹² Aldol condensation with the Li-enolate of α -alkoxyester **14** afforded the corre-

sponding product **15** in excellent yield. In the cases where alkylated glycolate esters **14** are not commercially available, they were prepared by alkylation of glycolic ester with the appropriate alkyl iodide in the presence of Ag_2O .¹³ Ionic reduction with triethylsilane in TFA¹⁴ and basic hydrolysis completed eventually the synthesis of **2**. The corresponding naphthalene derivatives **3** and the isomeric benzothiophenes **4** were prepared analogously, but using in step (f) 4-hydroxy-naphthalene-1-carbaldehyde or 7-hydroxy-benzo[*b*]thiophene-4-carbaldehyde, respectively.

Homochiral PPAR ligands **2**, **3**, and **4**, on the other hand, were synthesized using Evans' boron enolate methodology as depicted



Scheme 2. Reagents and conditions: (a) AcOH/HCl gas, 0 °C, 1 h, 60–90%; (b) $\text{POCl}_3/\text{CH}_2\text{Cl}_2$, reflux, 14 h, 60–90%; (c) NaCN/DMSO, 35 °C, 2 h, 90–98%; (d) NaOH/EtOH/water, 65 °C, 14 h, 60–85%; (e) BH_3/THF , rt, 14 h, followed by reflux in MeOH, 1 h, 80–95%; (f) $\text{Ph}_3\text{P}/\text{DIAD}/\text{toluene}$, rt, 2 h, 25–50%; (g) LDA/THF/hexane, –78 °C, 30 min, 70–98%; (h) Et_3SiH (10 equiv)/TFA, 0 °C, 3–14 h, 60–85%; (i) NaOH/EtOH/THF/water, rt, 2 h, 70–95%.



Scheme 3. Reagents and conditions: (a) $n\text{Bu}_2\text{BOTf}$, NEt_3 , CH_2Cl_2 , -78 to 0 °C, 3 h, 30–90%; (b) Et_3SiH , TFA, 14 h, 60–90%; (c) LiOH/THF , 35 °C, 2 h, 90–98%.

in Scheme 3.^{14,15} The control of absolute configuration at the α -position was close to perfect (routinely >95%). Similar ionic reduction as above and ensuing mild hydrolysis afforded the desired target in good yield.

All compounds were screened in PPAR α and γ binding (IC_{50}) and transactivation (EC_{50}) assays; selected compounds were also tested in PPAR δ assays.¹⁶ As can be seen from Table 1, most of the molecules turned out to be potent agonists at both receptors.

Table 1
Binding affinities (IC_{50}) and functional transactivation data (EC_{50}) of **2**, **3**, and **4** on human PPARs^{a,b}

| Compound No. | R ¹ | R ² , R ^{2'} | R ³ , R ^{3'} | R ⁴ | $\text{IC}_{50\alpha}$ (μM) | $\text{IC}_{50\gamma}$ (μM) | $\text{EC}_{50\alpha}$ (μM) (% effect) | $\text{EC}_{50\gamma}$ (μM) (% effect) |
|----------------------|---|----------------------------------|----------------------------------|-----------------|--|--|---|---|
| <i>rac</i> -2Aa | CH ₃ | H, H | H, H | H | 0.028 | 0.046 | 0.103 (168) | 0.059 (131) |
| <i>rac</i> -2Ba | CH ₃ CH ₂ | H, H | H, H | H | 0.022 | 0.007 | 0.027 (164) | 0.018 (100) |
| <i>rac</i> -2Ca | CH ₂ CH ₂ CH ₂ | H, H | H, H | H | 0.175 | 0.004 | 0.075 (123) | 0.012 (64) |
| <i>rac</i> -2Da | CH ₂ CH(CH ₃) ₂ | H, H | H, H | H | 0.239 | 0.003 | 0.048 (181) | 0.004 (63) |
| <i>rac</i> -2Ea | <i>n</i> -Hexyl | H, H | H, H | H | 0.120 | 0.002 | 0.249 (115) | 0.004 (85) |
| <i>rac</i> -2Ag | CH ₃ | OMe, H | H, H | H | 0.294 | 0.916 | 0.435 (101) | 1.615 (64) |
| <i>rac</i> -3Aa | CH ₃ | H, H | H, H | H | 0.061 | 0.113 | 0.131 (159) | 0.123 (98) |
| <i>rac</i> -3Ba | CH ₃ CH ₂ | H, H | H, H | H | n. d. | 0.030 | n. d. | n. d. |
| <i>rac</i> -3Ca | CH ₂ CH ₂ CH ₂ | H, H | H, H | H | 0.069 | 0.007 | 0.087 (56) | 0.016 (81) |
| <i>rac</i> -3Ah | CH ₃ | Me, H | H, H | H | 0.432 | 0.802 | 0.123 (114) | 0.716 (78) |
| (<i>S</i>)-2Aa | CH ₃ | H, H | H, H | H | 0.038 | 0.019 | 0.050 (156) | 0.021 (67) |
| (<i>S</i>)-2Ab | CH ₃ | H, H | H, H | CF ₃ | 0.053 | 0.023 | 0.002 (109) | 0.053 (132) |
| (<i>S</i>)-2Ac | CH ₃ | H, H | Me, Me | H | n. d. | 0.008 | 0.043 (?) | 0.011 (61) |
| (<i>S</i>)-2Ad | CH ₃ | H, H | H, H | <i>i</i> Pr | 0.045 | 0.002 | 0.020 (151) | 0.010 (53) |
| (<i>S</i>)-2Ae | CH ₃ | H, H | OMe, OMe | H | 0.048 | 0.003 | 0.061 (196) | 0.023 (44) |
| (<i>S</i>)-2Ba | CH ₃ CH ₂ | H, H | H, H | H | 0.053 | 0.021 | 0.027 (109) | 0.021 (63) |
| (<i>S</i>)-2Ca | CH ₂ CH ₂ CH ₂ | H, H | H, H | H | 0.393 | 0.002 | 0.013 (204) | 0.004 (25) |
| (<i>S</i>)-2Fa | CF ₃ CH ₂ | H, H | H, H | H | 0.060 | 0.003 | 0.555 (179) | 0.151 (119) |
| (<i>S</i>)-2Bb | CH ₃ CH ₂ | H, H | H, H | CF ₃ | 0.063 | 0.017 | 0.089 (43) | 0.009 (89) |
| (<i>S</i>)-2Ga | CH ₂ CHCH ₂ CH ₂ | H, H | H, H | H, H | 0.021 | 0.002 | 0.027 (108) | 0.032 (79) |
| (<i>S</i>)-2Bf | CH ₃ CH ₂ | H, H | H, H | Ph | 0.194 | 0.003 | 0.167 (92) | 0.431 (61) |
| (<i>S</i>)-2Gd | CH ₂ CHCH ₂ CH ₂ | H, H | H, H | <i>i</i> Pr | 0.037 | 0.005 | 0.016 (122) | 0.010 (56) |
| (<i>R</i>)-2Ba | CH ₃ CH ₂ | H, H | H, H | H | 2.370 | 2.68 | 1.91 (73) | 0.787 (81) |
| (<i>R</i>)-2Aa | CH ₃ | H, H | H, H | H | 4.610 | 1.44 | 0.358 (109) | 1.21 (65) |
| (<i>S</i>)-3Ba | CH ₃ CH ₂ | H, H | H, H | H | 0.198 | 0.036 | 0.011 (78) | 0.037 (72) |
| (<i>S</i>)-3Bb | CH ₃ CH ₂ | H, H | H, H | CF ₃ | 0.905 | 0.027 | 0.011 (135) | 0.021 (156) |
| (<i>S</i>)-3Ff | CF ₃ CH ₂ | H, H | H, H | Ph | 0.429 | 0.008 | 0.987 (79) | 0.038 (96) |
| (<i>R</i>)-3Aa | CH ₃ | H, H | H, H | H | 0.918 | 1.57 | 0.65 (92) | 0.122 (31) |
| (<i>S</i>)-4Aa | CH ₃ | H, H | H, H | H | 0.028 | 0.011 | 0.157 (174) | 0.033 (159) |
| (<i>S</i>)-4Ba | CH ₃ CH ₂ | H, H | H, H | H | 0.333 | 0.013 | 0.058 (89) | 0.007 (40) |
| Rosiglitazone (RG) | | | | | >10 | 0.45 | >10 | 0.45 (85) |
| Farglitazar (GW2570) | | | | | 0.633 | 0.001 | 0.284 (100) | 0.005 (252) |
| Fenofibric acid | | | | | 106 | 744 | 69 (11) | 217 (2) |

^a PPAR radioligand binding and functional transactivation (luciferase transcriptional reporter gene) assays were performed as described in Binggeli et al.²⁹

^b Effects are reported in relation to 2-(*S*)-2-(2-benzoyl-phenylamino)-3-[4-[2-(5-methyl-2-phenyl-oxazol-4-yl)-ethoxy]-phenyl]-propionic acid (Farglitazar, GW 262570) (100%, PPAR α) and 5-[4-[2-(5-methyl-2-phenyl-oxazol-4-yl)-ethoxy]-benzo[*b*]thiophen-7-ylmethyl]-thiazolidine-2,4-dione (Edaglitazone) (100%, PPAR γ).

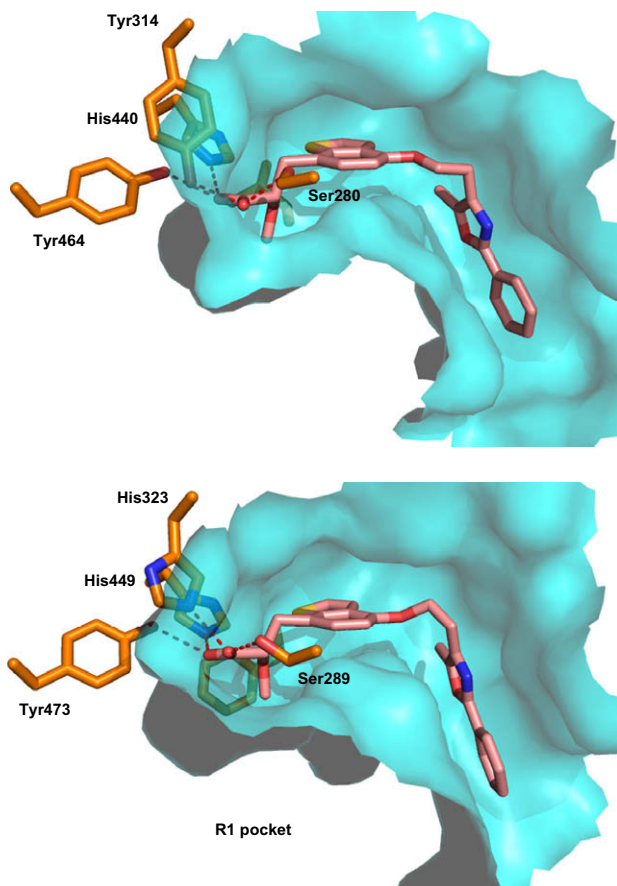


Figure 2. X-ray structures of (S)-2Aa bound to hPPAR α - (top) and γ -ligand binding domain (bottom).

Increasing length and size of R¹ tends to boost potency at the γ -isoform, whereas the opposite is true with respect to PPAR α . Branching is deleterious; unsaturation in the side chain, however, is well tolerated ((S)-2Ga, (S)-2Gd). As could be anticipated, (R)-isomers are almost inactive. The substitution pattern of the phenyl-oxazole influences the affinity only marginally, with the only exception

that ortho-substitution, in particular *o,o'*-disubstitution, abolishes activity completely.

To gain further insight into the binding mode we cocrystallized the ternary complex of the human PPAR α receptor ligand binding domain with compound (S)-2Aa and a receptor coactivator SRC-1 fragment.¹⁷ The structure was solved to a resolution of 2.2 Å and showed a clear electron density for the bound ligand.¹⁸ In addition, dual agonist (S)-2Aa was also cocrystallized with the ternary complex of the human PPAR γ receptor ligand binding domain with the agonist and a receptor coactivator SRC-1 fragment.¹⁹ This structure was solved to a resolution of 2.3 Å.¹⁸ The overall shape of this complex is very reminiscent of previously published PPAR α and γ complex structures with the AF2-helix in the agonist-type conformation. Within the ligand binding sites shown in Figure 2, the typical four strong hydrogen bonds between the ligand carboxylate and the Ser, His and Tyr residues of PPAR α and γ , respectively, can be identified (all H-bond distances ≤ 3.0 Å). Apart from the polar head group recognition, both binding sites are composed of predominantly hydrophobic side chains with limited solvent access in the central and tail region. The central benzothiophene linker designed to snugly fit into the protein cavity does its job as anticipated.²⁰

The two X-ray structures nicely allow rationalizing the observed reverse SAR trend with respect to R¹-extensions. While in PPAR γ a preformed pocket exists which can smoothly accommodate longer R¹ residues, the respective cleft in PPAR α is considerably smaller due to a sequence difference (Phe363(g) \leftrightarrow Ile354(a)). Very likely, the bulkier branched isoleucine clashes with larger R¹ residues resulting in a drop of binding affinity for this isoform.

(S)-2Aa, which has decent physicochemical properties, an excellent pharmacokinetic profile in several animal species²¹ and disposes of a well-balanced α/γ ratio was selected for further profiling.²² Figure 3 summarizes the results of an OGTT²³ after administering compound (S)-2Aa for 12 days to *db/db* mice at a dose of 0.3 or 3 mg/kg/d, respectively, in direct comparison with Rosiglitazone, and the effect on non-fasted plasma glucose levels. Even at ten times lower doses, (S)-2Aa compares very favorably with respect to both parameters very favorably with the reference insulin sensitizer Rosiglitazone (RSG).

(S)-2Aa was further profiled in a hyperinsulinemic euglycemic clamp study in Zucker *fa/fa* rats.²⁴ Figure 4 illustrates the robust ef-

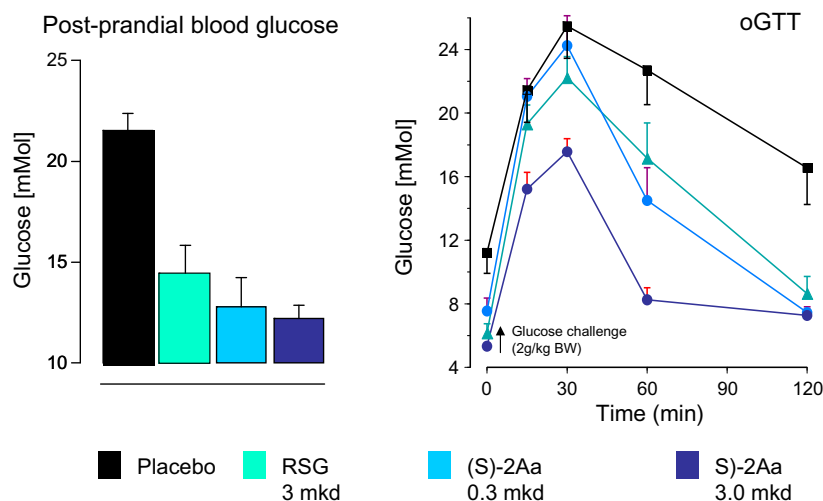


Figure 3. Oral Glucose Tolerance Test with (S)-2Aa and Rosiglitazone in *db/db* mice and effect on non-fasted plasma glucose. Post-prandial blood glucose levels (measured in the morning, after switch from dark to light cycle) in *db/db* mice. Data are expressed as mean \pm SEM, $N = 8$ per group. Oral Glucose challenge performed in overnight fasted *db/db* mice treated chronically. Last drug was administered (per gavage) on day prior to challenge. Data are expressed as mean \pm SEM, $N = 6$ /group.

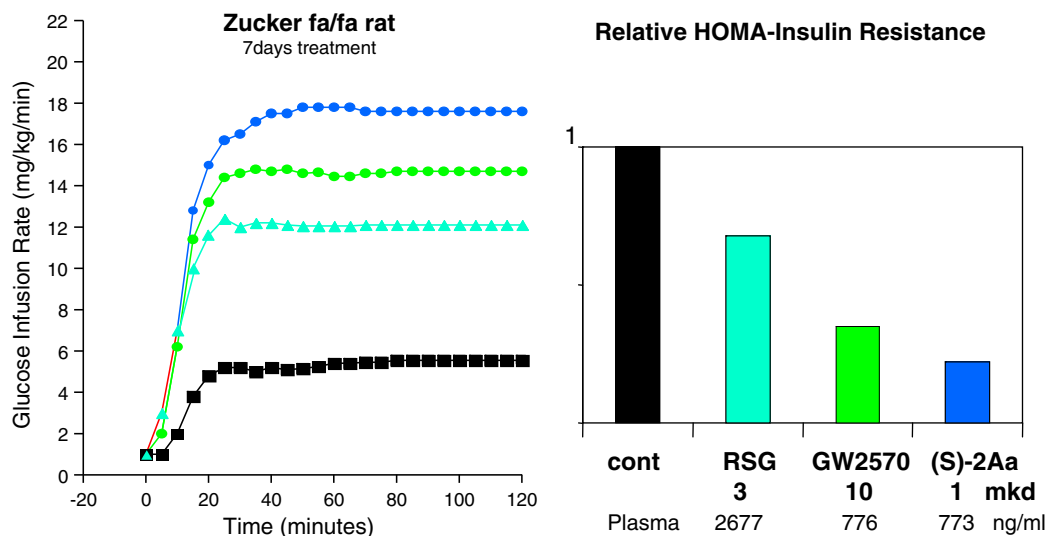


Figure 4. Euglycemic clamp study and insulin resistance index in *fa/fa* rats. GIR measured in *fa/fa* rats submitted to Euglycemic-Hyperinsulinemic clamp; data are expressed as mean values of $N = 5$ per group. SEM have not been included in the graph. HOMA-IR index was calculated from fasting plasma insulin and fasting blood glucose (FBG) levels measured at time 0 of the oGTT (prior to glucose challenge) in *fa/fa* rats. $\text{HOMA-IR index} = (\text{Fasting insulin (mU/ml)} \times \text{FBG (mM)})/22.5$.

fect, directly compared to 3 mg/kg/d of Rosiglitazone (RSG) and 10 mg/kg/d of Farglitazar (GW2570), respectively. The right panel shows the insulin-resistance indices^{25,26} as determined in the same model. Again, (S)-2Aa behaved very positively.

Last but not least, (S)-2Aa was also tested in different animal models of dyslipidemia. Figure 5 illustrates the data generated in human ApoA1-transgenic mice.²⁷ A robust increase of the amount of HDLc was observed, whereas the predominantly PPAR γ agonist

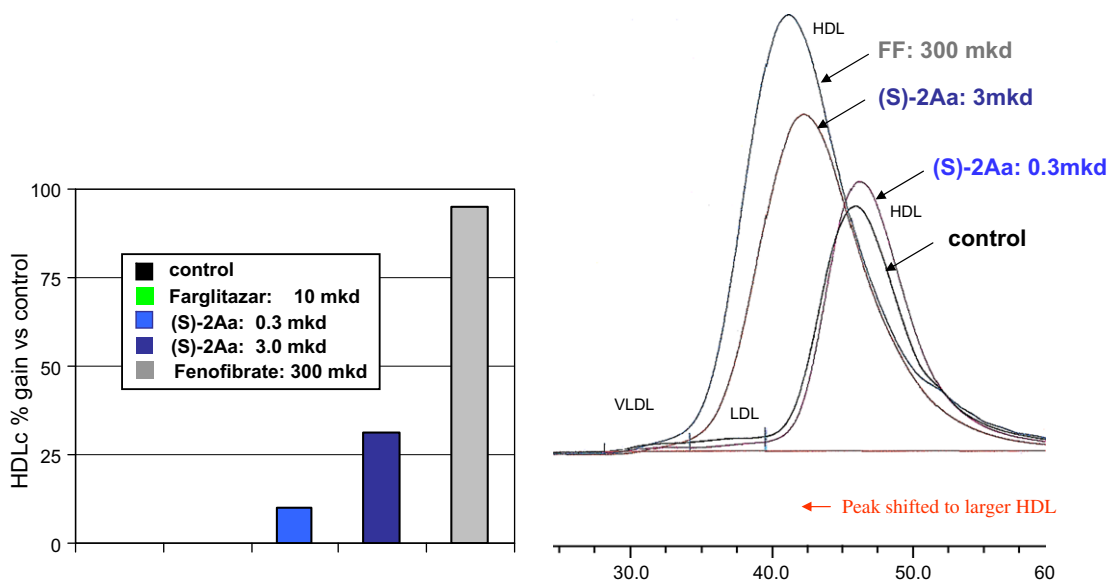


Figure 5. Effects on HDLc in human ApoA1-transgenic mice. Effects on HDLc measured in human ApoA1-transgenic mice after 12 days of treatment. Plasma lipid levels were measured by FPLC method from pooled plasma ($N = 8$ per group); data expressed as averaged values.

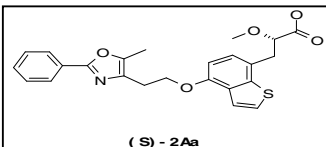
| | alpha-human | alpha-rat | alpha-mouse |
|--|------------------------|------------------------|------------------------|
| | EC50 (μM) | EC50 (μM) | EC50 (μM) |
|  <p>(S) - 2Aa</p> | 0.050 | 2.26 | 2.34 |

Figure 6. Species-dependence of PPAR α affinity of (S)-2Aa.

Farglitazar had no effect in this model. The classical PPAR α drug Fenofibrate was found to be even more active, albeit at 100–1000 times higher doses. The right panel shows the drug-induced size shift of the HDL-particles.

At first glance, this lipid-lowering effect does not seem to be too impressive. However, one has to keep in mind that compounds **2–4** exhibit in general intriguing species selectivity with respect to PPAR α . Figure 6 exemplifies this phenomenon for (**S**)-**2Aa**. Functional affinity drops almost two orders of magnitude with respect to the human receptor. Taking this into account, the observed in vivo effect is still remarkable; and the anticipation that the higher potency in primates will also translate into a much stronger pharmacodynamic effect turned out to be true. In (pre)diabetic rhesus monkeys, supposed to be one of the most predictive animal models, (**S**)-**2Aa** proved to be extraordinarily efficacious.²⁸ Based on these highly promising data (**S**)-**2Aa** was eventually selected as clinical candidate. Under the USAN name Aleglitazar it recently completed successfully clinical phase II studies.

Acknowledgments

The authors gratefully acknowledge Christian Bitsch, Stefan Bürlü, and Thomas Burger for chemical syntheses, Angele Flament and Astride Schnoebelen for in vitro testing, Urs Sprecher and Philippe Verry for in vivo testing, Bernard Gsell and Martine Stihle for protein preparation and crystallisation efforts, Dr. Manfred Kansy for physicochemical and Dr. Beate Bittner for in vitro toxicological and pharmacokinetic investigations and for in vivo screens.

References and notes

- Zhang, Z.; Burch, P. E.; Cooney, A. J.; Lanz, R. B.; Pereira, F. A.; Wu, J.; Gibbs, R. A.; Weinstock, G.; Wheeler, D. A. *Genome Res.* **2004**, *14*, 580.
- Steinmetz, A. C.; Renaud, J. P.; Moras, D. *Annu. Rev. Biophys. Biomol. Struct.* **2001**, *30*, 329.
- van Raalte, D. H.; Li, M.; Pritchard, P. H.; Wasan, K. M. *Pharm. Res.* **2004**, *21*, 1531.
- Feige, J. N.; Gelman, L.; Michalik, L.; Desvergne, B.; Wahli, W. *Prog. Lipid Res.* **2006**, *45*, 120.
- Cheng, A. Y. Y.; Leiter, L. A. *Diabetes Obes. Metab.* **2008**, *10*, 691.
- Leff, T.; Mathews, S. T.; Camp, H. S. *Exp. Diabetes Res.* **2004**, *5*, 99.
- Fredenrich, A.; Grimaldi, P. A. *Diabetes Metab.* **2005**, *31*, 23.
- Kuhn, B.; Hilpert, H.; Benz, J.; Binggeli, A.; Grether, U.; Humm, R.; Maerki, H. P.; Meyer, M.; Mohr, P. *Bioorg. Med. Chem. Lett.* **2006**, *16*, 4016.
- Goldstein, B. J.; Rosenstock, J.; Anzalone, D.; Tou, C.; Ohman, K. P. *Curr. Med. Res. Opin.* **2006**, *22*, 2575.
- Keindall, D. M.; Rubin, C. J.; Mohideen, P.; Ledoine, J.-M.; Belder, R.; Gross, J.; Norwood, P.; O'Mahony, M.; Sall, K.; Sloan, G.; Roberts, A.; Fiedorek, F. T.; DeFronzo, R. A. *Diabetes Care* **2006**, *29*, 1016.
- Goto, Y.; Yamazaki, M.; Hamana, M. *Chem. Pharm. Bull.* **1971**, *19*, 2050.
- Puentener, K.; Scalone, M. US 2005070714 2005070714, 2005.
- Hamad, A.-S. S.; Schinzer, D. *Phosphorus, Sulfur Silicon Relat. Elem.* **2000**, *158*, 187.
- Haigh, D.; Birrell, H. C.; Cantello, B. C. C.; Eggleston, D. S.; Haltiwanger, R. C.; Hindley, R. M.; Ramaswamy, A.; Stevens, N. C. *Tetrahedron: Asymmetry* **1999**, *10*, 1353.
- Gage, J. R.; Evans, D. A. *Org. Synth.* **1990**, *68*, 83.
- Selected EC₅₀ values (effects are reported in relation to (2-methyl-4-[4-methyl-2(4-trifluoromethyl-phenyl)-thiazol-5-ylmethylsulfanyl]-phenoxy)-acetic acid (GW 501516) whose activity was set to 100%): (**S**)-**2Aa**: 0.053 μ M (22%), (**S**)-**2Ba**: 0.117 μ M (100%), (**S**)-**2Ca**: 0.045 μ M (93%), (**R**)-**2Aa**: 2.71 μ M (29%), (**S**)-**2Ae**: 0.678 μ M (70%), (**S**)-**3Ba**: 0.169 μ M (64%), (**S**)-**4Aa**: 0.137 μ M (44%).
- Co-crystals of PPAR α -LBD with (**S**)-**2Aa** were obtained using a similar protocol as described in Burgermeister, E. et al. *Mol. Endocrinol.* **2006**, *20*, 809. Data have been collected in-house on a rotating anode ($\lambda = 1.5418 \text{ \AA}$) to a maximum resolution of 2.2 \AA . Crystals belong to the orthorhombic space group $P2_12_12_1$ with cell axes $a = 42.4$, $b = 76.1$, $c = 98.5 \text{ \AA}$. The structure was determined by molecular replacement using the chain A of the pdb entry 1K7I and subsequently refined. Difference electron density was used to place the ligand by real space refinement.
- The coordinates of the structures of compound (**S**)-**2Aa** crystallized with the human PPAR α and γ ligand domains were deposited to the Protein Data Bank (PDBid: PPAR α -3G8I, PPAR γ -3G9E).
- Co-crystals of PPAR γ -LBD with (**S**)-**2Aa** were obtained using an identical protocol as described in Burgermeister, E. et al. *Mol. Endocrinol.* **2006**, *20*, 809. Data have been collected in-house on a rotating anode ($\lambda = 1.5418 \text{ \AA}$) to a maximum resolution of 2.3 \AA . Crystals belong to the orthorhombic space group $P212121$ with cell axes $a = 53.9$, $b = 70.0$, $c = 88.5 \text{ \AA}$. The structure was determined by molecular replacement using the chain A of the pdb entry 1PRG and subsequently refined. Difference electron density was used to place the ligand by real space refinement.
- The corresponding phenyl compound, albeit in racemic form, exhibits, for example, an EC₅₀ value of 0.172 μ M at the alpha receptor.
- Selected PK data: total clearance: 6.2 ml/min/kg (rat), 1.6 ml/min/kg (cynomolgus monkey); bioavailability: 70% (rat), 68% (cynomolgus monkey); half-life: 4 h (rat), 12.9 h (cynomolgus monkey).
- Preparation of (**S**)-**2Aa**: (a) (**S**)-4-Benzyl-3-(2-methoxy-acetyl)-oxazolidin-2-one (16.97 g, 68.1 mmol) was dissolved under a stream of Argon in 120 mL of CH₂Cl₂, treated with 11.4 mL of triethylamine (1.2 equiv), and cooled down to $-78 \text{ }^\circ\text{C}$. 75 mL of 1 M *n*Bu₃BOTf in of CH₂Cl₂ was then slowly added, the reaction mixture warmed to 0 $^\circ\text{C}$, and recooled after 50 min to $-78 \text{ }^\circ\text{C}$. 4-[2-(5-Methyl-2-phenyl-oxazol-4-yl)-ethoxy]-benzo[b]thiophene-7-carbaldehyde (24.75 g, 68.1 mmol), dissolved in 300 mL of CH₂Cl₂, was then added within 2 h while keeping the temperature carefully at $-78 \text{ }^\circ\text{C}$. After another 30 min, the temperature was raised to 0 $^\circ\text{C}$ and the mixture stirred for 1 additional h. Quenching with icewater, extracting with AcOEt, washing with water and brine, drying over MgSO₄, and evaporation of all solvents, followed by flash chromatography (SiO₂, AcOEt/hexane = 1/1), yielded 95.87 g of (**S**)-4-benzyl-3-((2*S*,3*R*)-3-hydroxy-2-methoxy-3-[4-[2-(5-methyl-2-phenyl-oxazol-4-yl)-ethoxy]-benzo[b]thiophen-7-yl]-propionyl)-oxazolidin-2-one as yellow foam, slightly contaminated with another diastereomer; ISP MS: 613.1 (M+H⁺), 635.0 (M+Na⁺). (b) (**S**)-4-Benzyl-3-((2*S*,3*R*)-3-hydroxy-2-methoxy-3-[4-[2-(5-methyl-2-phenyl-oxazol-4-yl)-ethoxy]benzo[b]thiophen-7-yl]-propionyl)-oxazolidin-2-one (40.0 g, 65.3 mmol) was dissolved in 100 mL of trifluoroacetic acid and treated at 0 $^\circ\text{C}$ with triethylsilane (50 mL, 4.8 equiv). The reaction was then allowed to proceed for 18 h at ambient temperature. Pouring onto crashed ice/NaHCO₃, extracting with AcOEt, washing with water and brine, drying over MgSO₄, and evaporation of the solvents left the crude product which was purified by flash chromatography (SiO₂, AcOEt/hexane = 3/7) to give 29.0 g of (**S**)-4-benzyl-3-((*S*)-2-methoxy-3-[4-[2-(5-methyl-2-phenyl-oxazol-4-yl)-ethoxy]-benzo[b]thiophen-7-yl]-propionyl)-oxazolidin-2-one as white foam; EI MS: 596.4 (M⁺), 564.3 (M-MeOH⁺); ¹H NMR (300 MHz, CDCl₃): δ 2.40 (s, 3H), 2.78 (dd, $J = 9.6$, 13.5 Hz, 1H), 3.05 (t, $J = 6.6$ Hz, 2H), 3.25–3.31 (m, 3H), 3.41 (s, 3H), 3.91 (t, $J = 8.3$ Hz, 1H), 4.07 (dd, $J = 2.4$, 9.0 Hz, 1H), 4.37 (t, $J = 6.6$ Hz, 2H), 4.37–4.44 (m, 1H), 5.43 (t, $J = 6.5$ Hz, 1H), 6.75 (d, $J = 8.1$ Hz, 1H), 7.17–7.32 (m, 7H), 7.40–7.46 (m, 4H), 7.97 (br d, $J = 7$ Hz, 2H). (c) (**S**)-4-Benzyl-3-((*S*)-2-methoxy-3-[4-[2-(5-methyl-2-phenyl-oxazol-4-yl)-ethoxy]-benzo[b]thiophen-7-yl]-propionyl)-oxazolidin-2-one (29.0 g, 48.6 mmol) was dissolved in 340 mL of THF and treated at 0 $^\circ\text{C}$ with 118 mL of 1 N NaOH (2.5 equiv) and the reaction allowed to proceed for 1 h at ambient temperature, when TLC indicated the absence of starting material. The reaction mixture was poured onto crashed ice and extracted twice with EtOEt to remove the chiral auxiliary. The aqueous layer was then acidified with HCl to pH 1 and extracted again with AcOEt. The organic layer was washed with water, dried over MgSO₄, and the volume reduced i. v. to induce crystallisation. The first crop, obtained at $-10 \text{ }^\circ\text{C}$, yielded after washing with hexane and drying 17.39 g of (**S**)-2-methoxy-3-[4-[2-(5-methyl-2-phenyl-oxazol-4-yl)-ethoxy]-benzo[b]thiophen-7-yl]-propionic acid ((**S**)-**2Aa**) as white crystals; mp 146–47 $^\circ\text{C}$; C₂₄H₂₃N₁O₅S₁; theory%: C, 65.89; H, 5.30; N, 3.20; S, 7.33. Found: C, 65.53; H, 5.52; N, 3.23; S, 7.22; HR-MS: calcd 436.12242, found 436.12222; HPLC (Chiralpak-AD, 25 cm \times 4.6 mm, 90% heptane/10% EtOH/0.2% TFA): 99.4%; ¹H NMR (400 MHz, CDCl₃): δ 2.40 (s, 3H), 3.06 (t, $J = 6.4$ Hz, 2H), 3.21 (dd, $J = 7.8$, 14.5 Hz, 1H), 3.35 (dd, covered, 1H), 3.34 (s, 3H), 4.20 (dd, $J = 4.8$, 7.6 Hz, 1H), 4.35 (t, $J = 6.6$ Hz, 2H), 6.73 (d, $J = 8.0$ Hz, 1H), 7.15 (d, $J = 8.0$ Hz, 1H), 7.32 (d, $J = 5.6$ Hz, 1H), 7.39–7.47 (m, 3H), 7.48 (d, $J = 5.6$ Hz, 1H), 7.97 (br d, $J = 8$ Hz, 2H); ISN MS: 436.3 (M-H⁻); ¹³C NMR (150 MHz, CDCl₃): δ (ppm) 10.28, 26.16, 37.47, 58.75, 66.85, 79.99, 105.44, 121.32, 123.04, 124.21, 126.07, 126.10, 127.38, 128.73, 130.04, 130.50, 132.62, 141.56, 145.15, 153.26, 159.73, 174.78.
- Lestradet, H. *Ann. Med. Int.* **1980**, *131*, 103.
- Koopmans, S. J.; Radder, J. K. *Biol. Med. Rev.* **1996**, *5*, 31.
- Matthews, D. R.; Hosker, J. P.; Rudenski, A. S.; Naylor, B. A.; Treacher, D. F.; Turner, R. C. *Diabetologia* **1985**, *28*, 412.
- Duncan, M. H.; Singh, B. M.; Wise, P. H.; Carter, G.; Alaghband-Zadeh, J. *Lancet* **1995**, *346*, 120.
- Fournier, N.; Atger, V.; Paul, J. L.; Moatti, N. *Ann. Biol. Clin. (Paris)* **1995**, *53*, 209. Data will be published in due course.
- Binggeli, A.; Boehringer, M.; Grether, U.; Hilpert, H.; Maerki, H.-P.; Meyer, M.; Mohr, P.; Ricklin, F., Wo 2002092084, 2002.